Inversion of spectral absorption in the optically complex coastal waters of the Mid-Atlantic Bight

Oscar Schofield,[1] Trisha Bergmann,[1] Mathew J. Oliver,[1] Andrew Irwin,[1] Gary Kirkpatrick,[2] W. Paul Bissett,[3] Mark A. Moline,[4] and Cris Orrico[4]

[1] Recent advances in hydrologic optics offer the potential for quantitative maps of inherent optical properties, which can be inverted into optically significant constituents. During summer experiments in the Mid-Atlantic Bight (MAB) a procedure to invert bulk absorption measurements from off-the-shelf technology was developed. The inversion provides optical concentration estimates of phytoplankton, colored dissolved organic matter (CDOM), and detritus. Inversion estimates were validated against chlorophyll fluorescence, filter pad absorption, and phytoplankton pigment measurements. The inversion could account for up to 90% of the observed variance in particulates, CDOM, and detritus. Robust estimates for phytoplankton community composition could be achieved but required constraints on the inversion that phytoplankton dominate the red light absorption. Estimates for the composition, as indicated by spectral slopes, for CDOM and detritus were not robust. During the summer months in nearshore waters of the MAB, total absorption was almost equally associated (±10%) with phytoplankton, detritus, and CDOM, and the regions of variability were associated with major frontal boundaries. The variance between particulates, CDOM, and detritus varied spatially and with year; which precluded robust correlations. *INDEX TERMS:* 4847 Oceanography: Biological and Chemical: Optics; 4855 Oceanography: Biological and Chemical: Plankton; 4899 Oceanography: Biological and Chemical: General or miscellaneous; *KEYWORDS:* absorption, phytoplankton, bio-optics, water mass analysis

1. Introduction

[2] Traditional "conservative" parameters (e.g., temperature and salinity) have been used to track water masses for nearly a century but developing additional parameters from chemical signatures to extend water type identification and water mass analysis into multidimensional space is of great utility [*Tomczak*, 1999]. Such a capability would improve adaptive sampling strategies [*Robinson and Glenn*, 1999], allowing researchers to study how water masses evolve and optimize ocean observing networks.

[3] It has been suggested that traditional water mass markers might be complemented with standard biological measurements such as chlorophyll [*Tomczak*, 1999] as an additional dimension would improve resolving water types in parameter space. Chlorophyll is a logical choice for this additional discrimination dimension, as it the preeminent proxy for phytoplankton abundance and can be estimated relatively easily by satellites and in situ sensors. Fluorometry is a powerful in situ mapping approach; however, variability in the fluorescence quantum yields requires local calibration data for deriving any quantitative estimate. This is difficult as changes in the fluorescence quantum yield reflect sensitivities to both the incident spectral irradiance and overall phytoplankton physiology [*Kiefer*, 1973; *Cullen*, 1982; *Falkowski and Kiefer*, 1985], both of which can change on the timescale of hours to days [cf. *Falkowski and Raven*, 1997].

[4] Another potential variable might be colored dissolved organic matter (CDOM), which has been used successfully to calibrate mass transport [*Aarup et al.*, 1996; *Højerslev et al.*, 1996]. Most coastal systems reflect the optical contributions of numerous in-water constituents (water, phytoplankton, CDOM, detritus, and sediment). This optical complexity compromises the accuracy of the satellite-derived products [cf. *Kirk*, 1994; *Mobley*, 1994]; however, this complex matrix of materials provides a potential library of parameters that might be effective for discriminating water types if methods could be developed that provide reliable estimates of the optically significant constituents present.

[1]Coastal Ocean Observation Lab, Institute of Marine and Coastal Sciences, Rutgers University, New Brunswick, New Jersey, USA.
[2]Mote Marine Laboratory, Sarasota, Florida, USA.
[3]Florida Environmental Research Institute, Tampa, Florida, USA.
[4]Biological Sciences Department, California Polytechnic State University, San Luis Obispo, California, USA.

[5] Significant effort over the last decade has focused on measuring the spectral dependency of the in situ inherent optical properties (IOPs). The reliability in situ instrumentation that can measure the spectral IOPs is increasing [*Pegau et al.*, 1995; *Twardowski et al.*, 1999; *Chang and Dickey*, 1999; *Schofield et al.*, 1999; *Boss et al.*, 2001]. A major advantage of these parameters is that they can be inverted to provide weights for optically active components (e.g., water, colored dissolved organic matter (CDOM), phytoplankton, detritus, sediment, etc.). These optical weights are proportional to component concentration [*Roesler and Perry*, 1995; *Chang and Dickey*, 1999; *Schofield et al.*, 1999; *Gallegos and Neale*, 2002]. These inversion techniques are often based on estimating the total absorption using generalized spectral absorption shapes for one or more of the individual absorbing components or using absorption ratios of different wavelengths that vary in a predictable way according to the components present. While promising in theory, the accuracy of these inverted measurements have not been systematically assessed over the wide optical gradients present in the nearshore coastal ocean. Furthermore, the performance of inversion techniques that do not require any "optimized" local in situ data to derive the generalized shapes has yet to be assessed. Ideally, minimal "local" tuning should be applied to these inversion techniques as this would allow for a "global" mechanistic approach, which is particularly important in complex coastal waters where local empirical relationships are likely to be extremely variable.

[6] In this manuscript, we assess the application of a simple optical inversion method using off-the-shelf oceanographic equipment for deriving optical parameters and assess the utility of the derived optical parameters to differentiate water types in the coastal ocean. Our goal is to assess how much information can be inverted from absorption data given a fixed number of wavelengths, which can then be used to determine the "optical" state of nearshore coastal waters.

2. Methods

2.1. Field Data

[7] The field efforts were conducted at the Long-term Ecosystem Observatory (LEO) off the central coast of New Jersey [*Glenn et al.*, 1998, 2000; *Schofield et al.*, 2002] during the ONR-sponsored Hyperspectral Coastal Ocean Dynamics Experiments (HyCODE) and the Coastal Ocean Modeling and Observation Program (COMOP). The LEO system is a highly instrumented 30 by 30 km research site that represents a coupled model/observation system where real-time data and model forecasts are provided to optimize field sampling [*Glenn et al.*, 1998; *Schofield et al.*, 2002]. For bio-optical research, one advantage of the field site is that it ranges from very turbid estuarine waters to relatively clear offshore waters within the 30 km research box. These optical gradients reflect the variable contributions of many optically active constituents such as phytoplankton, sediments, CDOM, and detritus.

[8] The standard shipboard transects consisted of several 15−25 km cross-shelf transects. Specific transect lines and the locations of the stations were determined by the real-time data from ocean forecast models, ships, and satellites focused on characterizing coastal upwelling dynamics

[*Schofield et al.*, 2002]. At each station, vertical profiles of optical and physical data were collected using an integrated bio-optical package. The bio-optical package consisted of a WET Labs Inc. absorption/attenuation meter (ac-9), a Falmouth CTD, a profiling Satlantic spectral radiometer, and a HOBI Labs backscatter sensor (Hydroscat-6). The measurements of the inherent optical properties used in this study were collected using the standard nine wavelengths (412, 440, 488, 510, 555, 630, 650, 676, and 715 nm) of the WET Labs Inc. ac-9. At each station, the instrument was lowered to depth to remove air bubbles and the instrument was allowed to equilibrate with ambient temperature before data were collected. Only data from the upcasts were utilized. Data were averaged into 0.25 m depth bins for all subsequent analyses. The instruments were factory calibrated prior to the field season. Manufacturer recommended protocols (http://www.WET Labs Inc.com/otherinfo/ugftp.htm) were used to track instrument calibration throughout the field season. This included clean water, temperature, and salinity calibrations. Whenever possible daily water calibrations were conducted; however, sampling schedules did not always allow for a daily calibration. Under these circumstances the most recent water calibration was used. It should be noted that this period without a calibration was at most three days.

[9] A CDOM absorption mapping system was installed on the ship [*Kirkpatrick et al.*, 2003], which consisted of a liquid waveguide capillary cell (LWCC, World Precision Instruments, Inc.) coupled to a fiber-optic spectrometer (S2000, Ocean Optics, Inc.) and a fiber-optic xenon flash lamp (PS-2, Ocean Optics, Inc.). Water was pumped by miniature peristaltic pump (P625, Instech Laboratories, Inc.) through size fractionation and cross-flow filters (MicroKros, Spectrum Laboratories, Inc.) and then through the LWCC for optical density spectra measurements. A continuous underway water supply was provided by tapping the flow through the ship's fire suppression system. Details regarding the LWCC operation procedures are given by *Kirkpatrick et al.* [2003].

[10] At each ship occupied station, water was collected with Niskin bottles from both surface and bottom waters. Aliquots were filtered, under low vacuum (<10 cm Hg), through GF/F (Whatman) glass fiber filters to concentrate the particles for pigment and absorption determinations. Filters were placed into snap top vials and quick frozen in liquid nitrogen. Samples were stored at −80°C until later analysis. Filters were analyzed for photosynthetic and photoprotective pigment complements were determined using high-performance liquid chromatography (HPLC) according to procedures of *Wright et al.* [1991]. Filter pad absorption was measured on a laboratory spectrophotometer; spectra were corrected for the path length amplification factor according to the procedures outlined by *Roesler* [1998]. Detrital absorption was determined by methanol extraction of particulate material according to *Kishino et al.* [1985]. The detrital absorption was subtracted from particulate absorption to provide an estimate of phytoplankton absorption. For discrete CDOM spectra, water was filtered through a 0.2 micron Nucleopore filter, and measured on a spectrophotometer using a 5 cm long path length cuvette.

[11] A second in situ data set was collected using a bottom mounted winch that profiled an instrument package
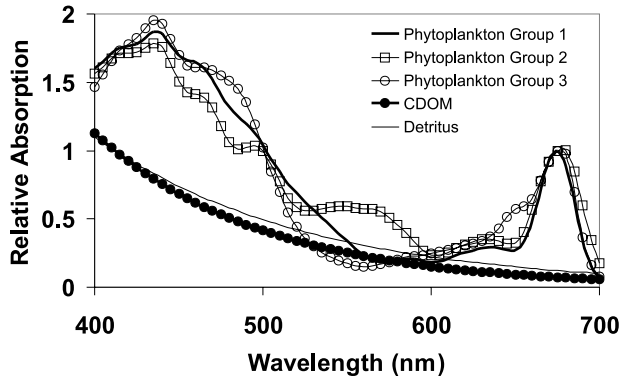
Figure 1. The input spectra used in the ac-9 inversion. Note that the spectral slopes for the CDOM and detritus were allowed to vary.

containing The Optical Profiler included a WET Labs ac-9 sampling at 6 Hz, and a two-wavelength backscatter/fluorometer HOBI Labs HydroScat-2 sampling at 2 Hz. The Optical Profiler was also profiled at 2 cm s^{-1}. The profiler was connected to the electro-fiber-optic LEO cable, allowing real-time data transmission back to shore. A detailed description of this system is provided by *Oliver et al.* [2004b]. This data set was complemented with a radioisotope data set [cf. *Oliver et al.*, 2004b] and that allowed us to assess the proportion of the water that was light saturated for photosynthesis.

2.2. Inversion of in Situ Absorption Data

[12] The optical signature inversion method (OSI) uses measured spectral absorption data collected from the ac-9 to calculate optical weight specific absorption coefficients for material present in the water column. The OSI model calculates optical weight specific coefficients (w_i) and exponential slopes (s, r) using a nonlinear constrained least-squares regression according to

$$a_{total}(\lambda) = w_1 a_{Phyto1}(\lambda) + w_2 a_{Phyto2}(\lambda) + w_3 a_{Phyto3}(\lambda)$$
$$+ w_4 a_{CDOM}(\lambda, s) + w_5 a_{Detritus}(\lambda, r) \qquad (1)$$

where $a_{total}(\lambda)$ is the total spectral absorption measured with the ac-9 (note that ac-9 provides an absorption that has already subtracted the contribution due to water), $a_{Phyto1}(\lambda)$, $a_{Phyto2}(\lambda)$, and $a_{Phyto3}(\lambda)$ are generalized spectral absorption of chlorophyll a-c, phycobilin, and chlorophyll a-b containing phytoplankton, respectively, and $a_{CDOM}(\lambda, s)$ and $a_{Detritus}(\lambda, r)$ are the spectral absorption of CDOM and detritus (Figure 1). The CDOM absorption (and detritus absorption) can be described as an idealized curve as a function of wavelength and exponential slope [*Kalle*, 1966; *Bricaud et al.*, 1981; *Green and Blough*, 1994],

$$a_{CDOM}(\lambda) = a_{CDOM} \exp[-s \bullet (\lambda - 412nm)] \qquad (2)$$

The exponential s parameter (unitless) is dependent on the composition of the CDOM present and is highly variable [*Carder et al.*, 1989; *Roesler et al.*, 1989]. Therefore it was necessary to allow the CDOM and detritus exponential slopes to vary spatially and temporally to achieve reasonable estimates. The initial exponential slopes of CDOM

were set to 0.010. The detritus exponential slope was initially set to 0.008. The slopes of the detrital curves (r) are lower [cf. *Kirk*, 1994] and detritus is described by equation (3),

$$a_{Detritus}(\lambda) = a_{Detritus} \exp[-r \bullet (\lambda - 412nm)] \qquad (3)$$

[13] The values of w_1, w_2, w_3, w_4, and w_5 are nonspectrally dependent scalar coefficients of these input spectra. We used fixed absorption spectra measured on laboratory cultures in order to ensure that inversion was completely independent from any spectral curves encountered in the field. Spectral phytoplankton curves were of averages of high-light- and low-light-acclimated phytoplankton spectra that were normalized to absorption at 676 nm. The spectral library used was taken from *Johnsen et al.* [1994] (Figure 1). While not optimal, we believe it was reasonable since the first-order determinant of spectral optical signals reflects the overall concentration of material rather than spectral characteristics of the materials present [*Barnard et al.*, 1998].

[14] We used two different inversion approaches, one with more constraints than the other. The minimal constraint OSI (OSI$_m$) only required that all solutions be positive (equation (4)), that CDOM and detritus absorption weights were equal in the red wavelengths of light (equation (5)), and that the CDOM exponential slope is steeper than the detrital slope (equation (6)). The assumption that the CDOM and detritus absorption is equal is artificial but we know that CDOM and detritus absorption is very low in the red wavelengths as both are exponentially decreasing curves. There are two artificial ways to ensure that the CDOM and detritus absorption do not dominate the red light absorption where phytoplankton absorption dominates. One method, more commonly used, is to set the magnitude of CDOM and detritus red absorption to a fixed low value. The second method is to anchor both curves to each other in the red, which allows the exponential slopes and amplitudes to be determined largely by the blue wavelength absorption. This second method allows the red light absorption of CDOM and detritus to be variable. The second OSI method (OSI$_c$) added constraints so that phytoplankton absorption dominated in the red wavelengths (equations (7) and (8)), and that minor phytoplankton communities in these waters (here chlorophytes) were never dominant (equations (9) and (10)). Specifically, the constraints on the OSI optimizations were:

$$w_1 a_{Phyto1}(\lambda), w_2 a_{Phyto2}(\lambda), w_3 a_{Phyto3}(\lambda), w_4 a_{CDOM}(\lambda, s),$$
$$w_5 a_{Detritus}(\lambda, r) \geq 0 \qquad (4)$$

$$w_4 a_{CDOM}(676nm, s) = w_5 a_{Detritus}(676nm, r) \qquad (5)$$

$$s \geq r \qquad (6)$$

$$w_1 a_{Phyto1}(676nm) \geq w_4 a_{CDOM}(676nm, s)$$
$$+ w_5 a_{Detritus}(676nm, r) \geq 0 \qquad (7)$$

$$w_2 a_{Phyto2}(676nm) \geq w_4 a_{CDOM}(676nm, s)$$
$$+ w_5 a_{Detritus}(676nm, r) \geq 0 \qquad (8)$$

$$w_1 a_{Phyto1}(\lambda) \geq w_3 a_{Phyto3}(\lambda) \qquad (9)$$

$$w_2 a_{Phyto2}(\lambda) \geq w_3 a_{Phyto3}(\lambda) \qquad (10)$$
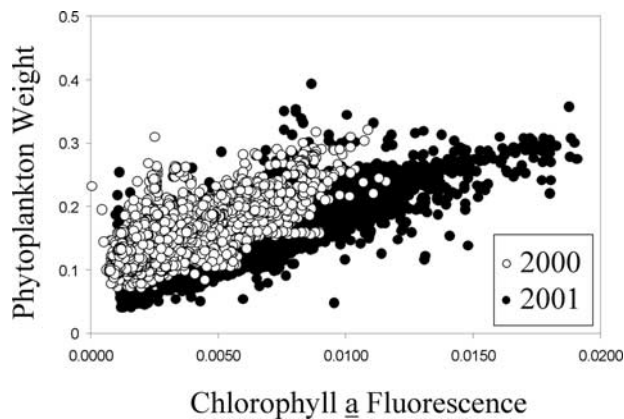
Figure 2. The relationship between chlorophyll *a* fluorescence measured with a HOBI Labs hydroscat-6 and the estimated phytoplankton weight during the summers of 2000 and 2001. The phytoplankton weight was inverted from ac-9 data using the OSI_c approach. The R^2 for summer 2000 and 2001 are 0.54 and 0.61, respectively.

[15] These assumptions were based on 5 years of experience in coastal New Jersey waters spanning both the nearshore and offshore. It should be noted that the OSI_m and OSI_c inversion methods using the same assumptions have been successfully used in both the oligotrophic Gulf of Mexico and the southern basin of Lake Michigan (unpublished data). When the OSI method (OSI_m and OSI_c) did not converge on a solution, the data were omitted from the later analysis (<5% of the total New Jersey data set). This generally reflected noise in the ac-9 data most often in near surface waters, presumably related to air bubbles, which interfered with natural inflections in the absorption curve. Of all the constraints, the requirement that green algae were always less abundant than chlorophyll *c* and phycobilin containing algae was admittedly the most artificial. However, running the inversion without the constraint greatly compromised the efficacy of the inversion for the overall phytoplankton absorption spectra. Omitting the chlorophytic algae also compromised the efficacy of the OSI method (data not shown). Phytoplankton pigment concentrations from discrete measurements during this study also confirmed that this assumption was valid as it was also confirmed a background population of green algae was detectable [*Moline et al.*, 2004]. To assess the stability of the OSI, random noise was introduced into the ac-9 spectra. For this analysis we added +0.005 m^{-1} to the data randomly across all wavelengths. Results indicated that there was no spectral bias and the quantitative impact was less than 1%.

3. Results and Discussion

3.1. Verification of the Derived Optical Products

[16] OSI-derived particulate, detrital, and phytoplankton loads were compared to three independent data sets that included stimulated chlorophyll fluorescence, phytoplankton filter pad absorption measurements, and HPLC phytoplankton pigment concentrations. All three data comparisons suggested that the OSI method provided reasonable estimates of particulate, phytoplankton, detritus, and CDOM optical weights.

3.1.1. Fluorescence

[17] The ac-9-derived phytoplankton absorption and stimulated in situ chlorophyll fluorescence were positively and linearly related to each other (Figure 2). The derived phytoplankton absorption was significantly correlated (p < 0.05) with fluorescence and could explain 54% and 61% of the variance in the summers 2000 and 2001, respectively. The linear relationship between the fluorescence and derived phytoplankton weight was notable given that the majority of the data were collected in Case 2 waters where phytoplankton are not necessarily the dominant optical signal (see below). Secondarily a significant proportion of the phytoplankton communities were light saturated for photosynthesis and thus fluorescence quenching was significant [*Falkowski and Kiefer*, 1985] (Figure 3). This quenching contributed to the variance in the correlation between the OSI-derived phytoplankton optical weights and chlorophyll fluorescence measurements. Xanthophyll pigment cycling [*Demmig-Adams*, 1990; *Owens et al.*, 1993] and photoinhibition [*Prasil et al.*, 1992; *Nickelsen and Rochaix*, 1994; *Critchley*, 1994] often results in almost a 100% change in fluorescence quantum efficiency [*Falkwoski and Kiefer*, 1985; *Kroon*, 1994]. The variable fluorescence quantum yield compromises the accuracy of using fluorescence to estimate chlorophyll *a* biomass, the OSI phytoplankton estimates may be more desirable than the commonly used chlorophyll fluorometer because it is not subject to physiological variability. IOP sensors are now becoming operationally viable for the wider oceanographic community, inverted optical data will improve our ability for making quantitative biomass maps.

3.1.2. Filter Pad Absorption

[18] The OSI results were compared to 240 filter pad samples that spanned the period of the field effort (Figures 4 and 5). For OSI_m, quantitative agreement with discrete samples for particulates was good with the R^2 ranging from 0.8 to 0.5 for wavelengths lower than 680 nm except in the wavelengths associated with carotenoid and phycobilin absorption (530 to 600 nm) (Figure 4a). The R^2 dropped to 0.3 for wavelengths greater than 680 nm. The average slope between the measured and predicted absorption ranged 1.2 to 0.5. Given the variance within the correlations, the average slope was rarely significantly different than one. The OSI_m could account for 70% of the variance in measured phytoplankton spectra except for the wavelengths associated with phycobilin absorption at wavelengths spanning from 530 nm to 600 nm (Figure 4b). The R^2 dropped for wavelengths greater than 680 nm. Average slopes between measured and predicted phytoplankton absorption were insignificantly different from one except in the low blue wavelengths (<415 nm) of light where phytoplankton absorption were overestimated by as much 20% (Figure 4b). OSI-derived detritus spectra could account for 70% of the variance in the absorption in the blue wavelengths of light (Figure 4c), but the R^2 dropped off at the higher wavelengths because of the low signal to noise associated with the exponential decline in detrital absorption with increasing wavelength. The CDOM absorption was significantly overestimated. In the blue wavelengths, this over estimate was 35% but increased to a factor of 2 in the
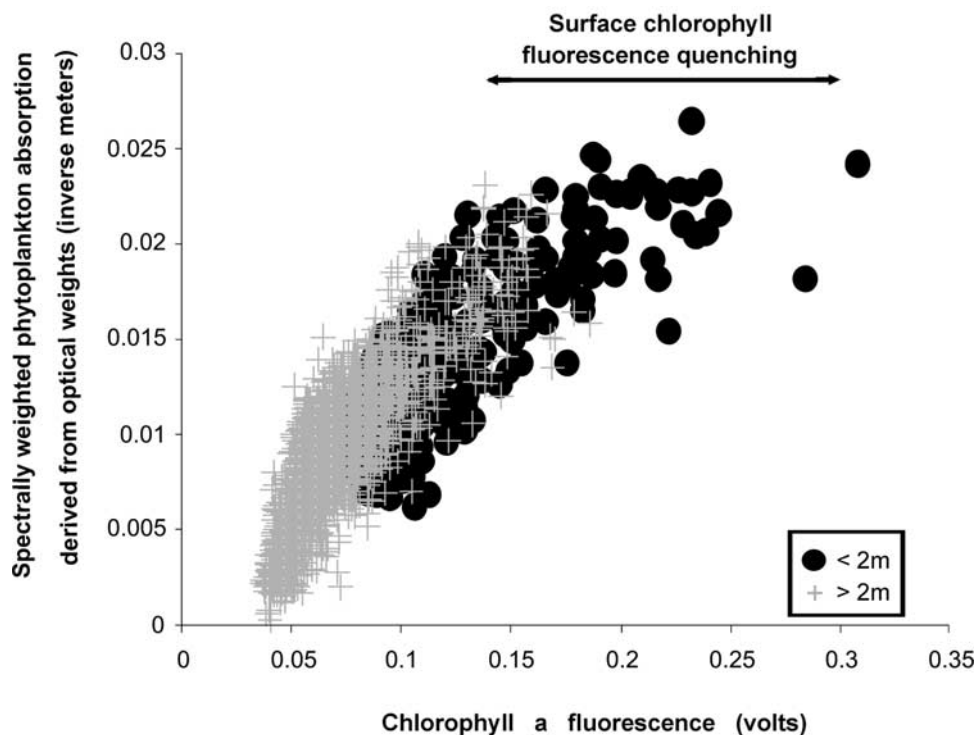
Figure 3. The relationship between chlorophyll for fluorescence and the OSIc-derived spectrally weighted absorption for phytoplankton communities at the Optical Profiler. Note that the nonlinearity between phytoplankton absorption and chlorophyll fluorescence measurements occurs in surface waters during periods of light saturation as a result of fluorescence quenching, which reflects a lower fluorescence quantum yield. Light saturation was determined with radio isotope productivity measurements [*Oliver et al.*, 2004b] were made on discrete water samples collected at the Optical Profiler.

green orange wavelengths of light (Figure 4d); however, the OSI_m-derived CDOM absorption could account 88% of the variance in the measured CDOM absorption in the blue wavelengths of light. Similar to the detritus the R^2 decreased with increasing wavelength because of decreasing signal to noise.

[19] For the OSI_c the quantitative agreement between measured and modeled particulate spectra was good, with the R^2 ranging from 0. 5 to 0.9 with low values associated with wavelengths greater than 680 nm (Figure 5a). The slope between the measured and modeled particulate spectra ranged from 1.2 to 0.8 depending on wavelength (Figure 5a) and the variance was reduced from the OSI_m approach especially in the wavelengths associated with phycobilin and carotenoid absorption (530–580 nm). For the majority of the wavelengths, the deviations of the average slope from 1 were rarely statistically significant (Figure 5a). Quantitative agreement decreased in the red wavelengths of light where signal was low. Results indicate that the derived particulate spectra could be quantitatively derived from the ac-9 with minor spectral biases despite that only idealized spectral absorption shapes were used. Like the particulate spectra, the agreement for the OSI and measured phytoplankton spectra were good (Figure 5b). The largest mismatches were in the blue wavelengths of light but 70–80% of the observed variance in the measured spectra were described by the OSI_c and as with the particulate spectra the errors were lower compared to the OSI_m method.

Quantitative estimates for detritus were good (Figure 5c), but accuracy dropped in the higher wavelengths because of low detrital absorption. The OSI_c method showed no improvements over the OSI_m method for predicting CDOM absorption, with the overall CDOM absorption being overestimated significantly (Figure 5d). For both OSI_m and OSI_c the spectral slope of the CDOM was underestimated especially when discrete samples indicated high slopes (Figure 6).

[20] In our approach, the input spectra for the OSI were based on laboratory data [*Johnsen et al.*, 1994] and theoretical curves, so the OSI methods could undoubtedly be improved by customizing the input spectra for any particular location. Our goal, however, was to assess what could be derived using no local input data. The relative particulate spectra derived by the OSI_c approach overestimated absorption at wavelengths of peak phytoplankton absorption (420–540 and 660–680 nm). This is consistent with the well-documented package effect, where absorption spectra are "flattened" when pigment packaged within a cell [*Morel and Bricaud*, 1986]. The package effect is greatest in the wavelengths of maximal absorption and increases with increasing cell size and cellular concentration of pigment. In higher-chlorophyll waters nearshore, water samples revealed high populations of large net diatoms [*Moline et al.*, 2004], which have been found to be greatly affected by the pigment package effect [*Bricaud et al.*, 1995]. Filter pad measurements support the hypothesis that
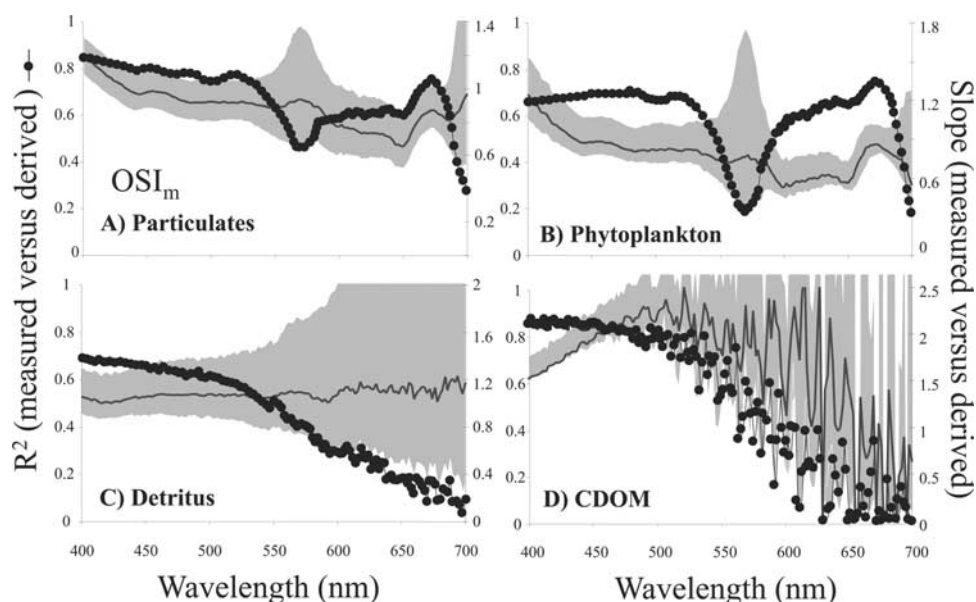
Figure 4. Comparison of measured and modeled particulate, phytoplankton, detritus, and CDOM absorption using the minimal constraint OSI method. The measured data represent absorption spectra made for either filter pads or dissolved organics on discrete samples. The modeled data represent the absorption spectra predicted from the inverted ac-9 data. Data were pooled for both years and were linearly regressed at each wavelength providing both the slope and R^2 for each wavelength. The absolute differences between ac-9-derived and filter pad determinations for (a) particulates, (b) phytoplankton, (c) detritus, and (d) CDOM absorption are presented. The grey shadow around the slope represents the standard deviation.
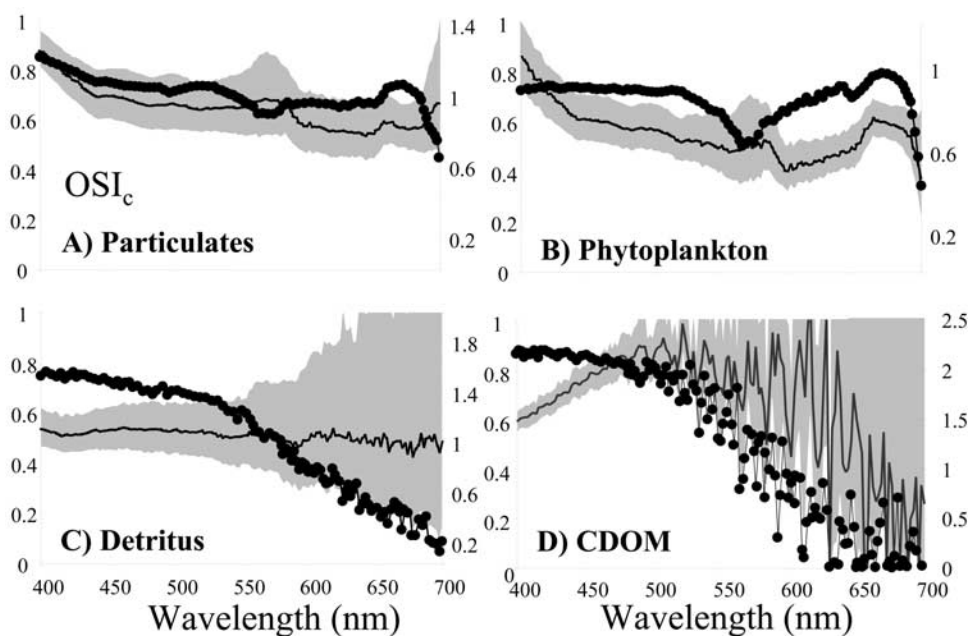

Figure 5. Comparison of measured and modeled (a) particulates, (b) phytoplankton, (c) detritus, and (D) CDOM absorption using the OSI_c method. The measured data represent absorption spectra determined from filter pads or discrete samples for colored dissolved organics. Data were pooled for both years and were linearly regressed against measured absorption spectra at each wavelength providing both the slope and R^2 for each wavelength. The grey shadow around the slope represents the standard deviation.
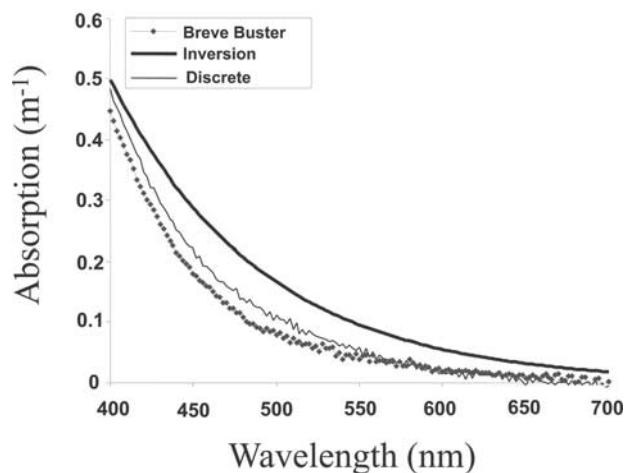
Figure 6. Comparison of CDOM spectral absorption estimated by the OSI$_c$ and measured with a flow through BreveBuster [*Kirkpatrick et al.*, 2003] and on a discrete sample.

phytoplankton were highly packaged as the specific absorption at 676 nm was consistently lower (0.017 m^2 mg chla^{-1}) than in low-chlorophyll offshore waters where populations were dominated by picoplankton. Therefore as the majority of the data collected represented nearshore stations, the package effect could account for much of spectral differences in the derived spectra. The pigment package effect has a proportionally larger impact on the wavelengths of maximum phytoplankton absorption.

[21] The spectral mismatch resulting from the highly peaked phytoplankton contributed to the overestimated CDOM absorption. This is associated with the high pigment absorption in the blue and red wavelengths of light. Given the OSI requirement that phytoplankton dominate the red absorption peak, a flatter phytoplankton input absorption spectra would result in 1) lower the overall CDOM and detrital estimates in the blue wavelengths and 2) steeper estimates in the CDOM exponential slope. This would argue that laboratory spectra should not be used in the inversion of field data; however, it was the highly peaked pigment shoulders that allowed phytoplankton community composition to be determined. Until more wavelengths are available to allow researchers characterize both composition and pigment packaging researchers will be forced to prioritize their needs. This shortcoming will improve in the coming years as in situ hyperspectral sensors are actively being developed by the community.

3.1.3. Phytoplankton Pigments

[22] To further assess the phytoplankton absorption inversion estimates, we examined how well the presence of the three spectral classes of phytoplankton could be determined (Figure 7). Using accessory pigment data and the ChemTax program [*Mackey et al.*, 1996, 1998] we estimated the proportion of total chlorophyll a associated with the three major spectral classes of phytoplankton. The inverted phytoplankton estimates from the OSI$_c$ method were significantly correlated (p < 0.00) with the ChemTax estimates of chlorophyll c and phycobilin-containing phytoplankton (Figure 8). There was no success in predicting the distribution of chlorophyll b, but this is consistent

with the independent findings that they were a rare component of the phytoplankton community at LEO and thus had insignificant contributions to the optical signals [*Moline et al.*, 2004]. The OSI$_m$ approach had no success in predicting the phytoplankton community composition.

[23] Overall results from the OSI show that currently available off-the-shelf technology can provide reasonable estimates of the major optical constituents (CDOM, detritus, particles, and phytoplankton) in Case 2 waters. While the precise phytoplankton community composition was difficult to delineate, the most dramatic gradients in phytoplankton composition could be described given constraints that maximized the phytoplankton absorption in the red wavelengths of light. Improving this and similar inversion methods will require spectral resolutions greater than nine wavelengths, ideally, at the wavelengths associated with phytoplankton accessory pigments [*Jeffrey et al.*, 1997]. Increased spectral resolution would also allow a variety of spectral pattern recognition methods to be applied [*Millie et al.*, 1997; *Schofield et al.*, 1999; *Kirkpatrick et al.*, 2000; *Millie et al.*, 2003], which will increase our ability to discriminate the major spectral classes of phytoplankton and even specific phytoplankton taxa [*Millie et al.*, 2002; O. Schofield et al., Studying harmful algal blooms in a dynamic environment: How can optics help the field-going sample-poor biologist?, in *Application of Optics to Studying Harmful Algal Blooms*, edited by M. Babin and J. J. Cullen, United Nations Educational, Scientific, and Cultural Organization, Paris, manuscript in review, 2004]. Many of these approaches require spectral resolutions of 2−3 nm [*Roelke et al.*, 1999] so developing hyperspectral instrumentation will be key to improving optical discrimination techniques for coastal waters. Despite shortcomings, this approach appears very promising as the distributions of the major absorbing components at LEO corresponded to large-scale hydrographic changes [*Chang et al.*, 2002; *Johnson et al.*, 2003].

3.2. Summer Distributions in the Optical Products

[24] Derived optical products were variable in space and time, as significant differences were observed between the two summer experiments. Optical parameters (discussion from here refers to the OSI$_c$ inverted estimates) showed robust relationships to hydrography, suggesting that the derived optical products reflected natural variability (Figures 9−10).

3.2.1. Summer 2000

[25] In summer 2000, storm events and a low-salinity plume dominated the hydrography [*Chang et al.*, 2002; *Johnson et al.*, 2003]. The highest concentrations of phytoplankton, CDOM, and detritus were found above the summer thermocline, which was found between 7 and 10 m (Figures 8). Phytoplankton, CDOM, and detritus equally dominated absorption in the blue wavelengths, except in the thermocline, where phytoplankton absorption dominated (Figure 8a), and in offshore bottom waters where CDOM and detritus absorption dominated (Figures 8b and 8c). The net effect is pronounced blue light absorption, and corresponding low blue reflectance leading to the pristine green coastal waters that grace the New Jersey shore. While the relative absorption of phytoplankton, CDOM, and detritus were generally inversely related to each other, the
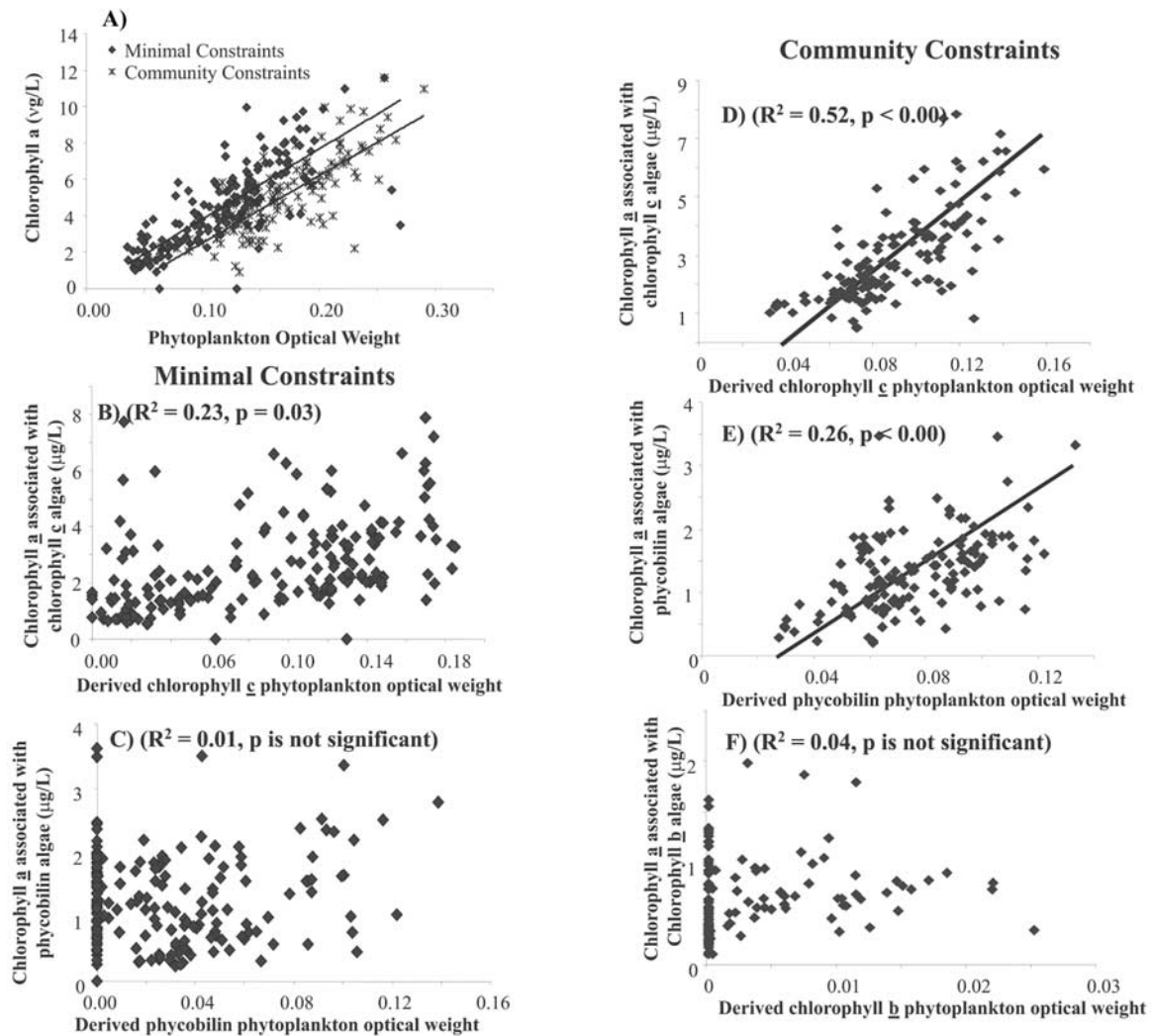
Figure 7. Comparison of the amount of phytoplankton absorption and measured chlorophyll *a* associated with the three major spectral classes of phytoplankton during summers 2000 and 2001. The amount of chlorophyll *a* associated with each spectral class of phytoplankton was calculated via CHEMtax using the accessory pigment data measured via high-performance liquid chromatography. (a) Relationship between measured chlorophyll *a* to the OSI_m and OSI_c procedures. (b) The absorption of chlorophyll *c* containing algae estimated with the OSI_m and the chlorophyll *a* associated with chromophytic algae. (c) The absorption of phycobilin containing algae estimated with the OSI_m and the chlorophyll *a* associated with phycobilin containing algae. (d) The absorption of chlorophyll *c* containing algae estimated with the OSI_c and the chlorophyll *a* associated with chromophytic algae. (e) The absorption of phycobilin containing algae estimated with the OSI_c and the chlorophyll *a* associated with phycobilin containing algae. (f) The absorption of chlorophyll *b* containing algae estimated with the OSI_c and the chlorophyll *a* associated with chlorophytic containing algae.

observed variances covaried spatially with the highest variances observed 15–20 km offshore throughout the water column (Figures 8d, 8e, and 8f). The variance was highest just offshore of an observed salinity front that was associated with the Hudson River [see *Chang et al.*, 2002, Figures 8b and 8c; see also *Johnson et al.*, 2003]. The offshore side of the front was impacted by a tidally induced convergence zone [*Schofield et al.*, 2002] that could be delineated with using surface current radar measurements [*Chang et al.*, 2002; *Schofield et al.*, 2002]. On the incoming tide, material accumulated offshore of the southern flowing jet, which was then dispersed upon reversal of

the tide. This convergence/divergence feature was persistent during the experiment to such a degree that it was possible to adaptively sample the feature [*Schofield et al.*, 2002].

3.2.2. Summer 2001

[26] Summer 2001 was dominated by alternating upwelling and downwelling favorable winds that resulted in strong stratification. Phytoplankton distributions (Figure 9a) were highly correlated with temperature (data not shown) and were higher than in summer 2000. Consistent with summer 2000, the optical estimates for CDOM and detritus were highest in surface waters above the 10m thermocline. During this upwelling summer season, phytoplankton
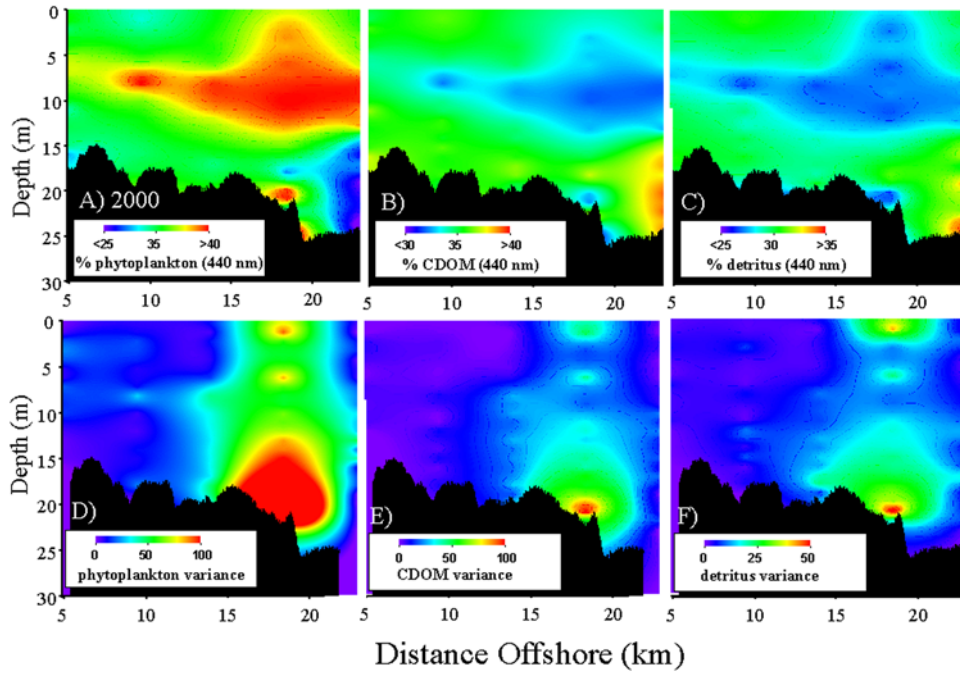
Figure 8. The spatial variability in the percent mean absorption at 440 nm for (a) phytoplankton, (b) CDOM, and (c) detritus during summer 2000. The pooled variances in the percent mean absorption at 440 nm for (d) phytoplankton, (e) CDOM, and (f) detritus is also presented. Note the scale changes.

concentrations dominated the total absorption in the surface waters above the thermocline. CDOM and detritus absorption were highest in bottom waters (Figure 9b). In contrast to the CDOM absorption and variance, which were highest offshore, the relative detrital absorption was highest in the nearshore bottom waters below the thermocline (Figure 9c). The variance was highest for all three parameters at the interface between the phytoplankton dominated surface waters and CDOM dominated bottom waters (Figures 9d–9f). The alternating onshore and offshore
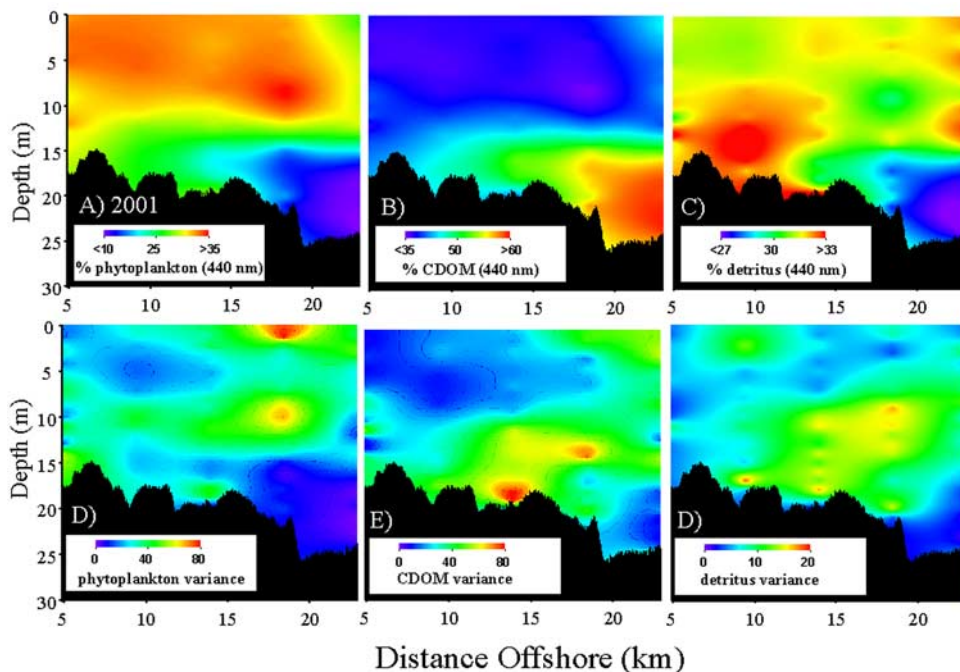

Figure 9. The spatial variability in the percent mean absorption at 440 nm for (a) phytoplankton, (b) CDOM, and (c) detritus during summer 2001. The pooled variances in the percent mean absorption at 440 nm for (d) phytoplankton, (e) CDOM, and (f) detritus is also presented. Note the scale changes.
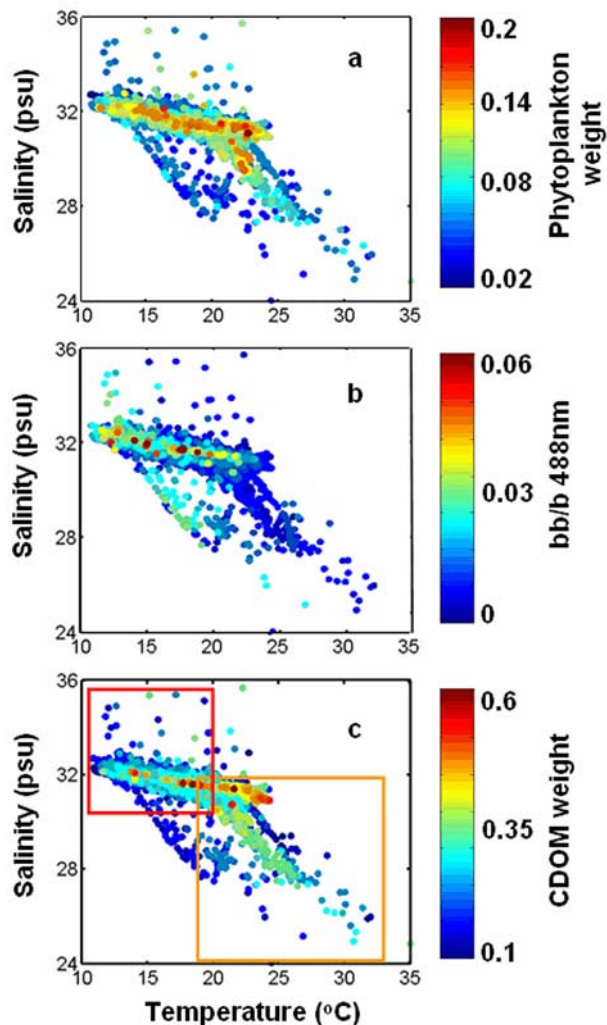
Figure 10. The relationship between temperature, salinity, and optical parameters using the combined databases collected during summers of 2000 and 2001 (n > 15,000). (a) The relationship between phytoplankton optical weight, temperature, and salinity. (b) The relationship between backscatter to total scattering ratio, temperature, and salinity. (c) The relationship between CDOM optical weight, temperature, and salinity. The red box outlines the general properties found in bottom waters at the LEO site. Summer 2000 was impacted by heavy rainfall, and a large low-salinity plume was observed during the experiment. The orange box outlines the general properties associated with the buoyant plume.

transport of the cold bottom waters transported optically distinct waters into our study site. The total absorption in these cold bottom waters was dominated by CDOM absorption with only minor contributions from phytoplankton or detritus. Detrital absorption was highest in bottom waters, which correlated with discrete measurements that indicated the presence marine snow and transparent exopolymer particles [*Alldredge and Silver*, 1988; *Alldredge et al.*, 1993; *Passow et al.*, 1994]. This cold offshore water was also delineated by the backscattered to total scattered light (b_b/b) ratio. This ratio reflects both the size and the refractive index of the

particles [*Twardowski et al.*, 2001; *Boss et al.*, 2001]. These waters often contain both resuspended sediments, which are often a fine-sand/silt mix [*Craghan*, 1995] and/or degraded material from picoplankton-dominated communities found offshore [*Moline et al.*, 2004]. The net effect is that both of these variables will increase the b_b/b ratio. Smaller phytoplankton cells have enhanced backscatter because of the size [cf. *Mobley*, 1994], and fine silts tend to have enhanced backscatter cross sections based on changes in the refractive index (on average 1.05 for phytoplankton to 1.25 for inorganic particles). Offshore bottom waters were consistently delineated by the ratio b_b/b ratio (data not shown) and thus were positively correlated with the CDOM slope.

3.2.3. Delineating Water Masses

[27] Phytoplankton optical loads were positively correlated with the concentration of detritus and CDOM; however, no robust predictive empirical relationships could be derived. The positive relationship between CDOM and phytoplankton is consistent with many studies [cf. *Nelson and Siegel*, 2002] but given the proximity to land it was not possible to infer the source of material present. On this shallow continental shelf high-frequency wind mixing and numerous upwelling events [*Glenn et al.*, 2004] minimize phytoplankton nutrient limitation allowing for high growth rates. Storm events lead to the resuspension of benthic algal communities into the water column. Finally the local rivers generally have high phytoplankton concentrations. For CDOM, the sources include cellular exudation/lysis/defecation [*Kalle*, 1966; *Bricaud et al.*, 1981; *Guixa-Boixeru et al.*, 1999], resuspension from sediments [*Chen*, 1999; *Komada et al.*, 2002] and inputs of water ladened with terrestrially derived humics/fulvics [*Blough et al.*, 1993; *Vodacek et al.*, 1997].

[28] Combining the optical data sets with hydrographic data may assist in differentiating water masses in the Mid-Atlantic Bight (MAB) (Figure 10). Phytoplankton optical concentrations were in found in water masses where the temperatures ranged from 12 to 25°C and the salinities ranged from 34 to 27 PSU (Figure 10). This effectively covered the range of hydrographic conditions observed and thus phytoplankton concentration did not show great utility in delineating water masses (Figure 10). The CDOM concentrations were highest when water temperatures ranged from 18 to 25°C and the salinities ranged from 32 to 26 PSU (Figure 10). Highest values were observed for salinities less the 31 PSU, which were largely associated with surface and buoyant river plumes [*Johnson et al.*, 2003, Figure 11]. In contrast the highest values of the b_b/b ratio were found in lower water temperatures (10 to 17°C) associated with cold bottom waters. These optical proxies may provide a means for extending traditional water type identification and water mass analysis into multidimensional space [*Tomczak*, 1999; *Oliver et al.*, 2004a]. These proxies should only be applied when their transformation rates are slower than the process being studied. The rate of change of these inverted optical proxies is on the order days to weeks [*Falkowski and Raven*, 1997; *Nelson et al.*, 1998; *Nelson and Siegel*, 2002; *Twardowski et al.*, 2001]. This is a great improvement over fluorometric estimates of biomass, which can change on the timescale of hours, and is currently the instrument of choice for most hydrographic packages. Given this we

recommend that IOP sensors be routinely incorporated into standard hydrographic surveys.

4. Conclusions

[29] Inversion of absorption data measured using off the shelf technology is possible and shows great promise. These and similar inversion approaches can be applied to optically complex Case 2 waters. Particulate spectra were derived with great efficacy. Deriving phytoplankton spectra was more difficult but achievable. This will provide the marine ecologist a key technology to map specific phytoplankton taxa over ecologically relevant spatial temporal scales. The absorption during the summer upwelling season in the nearshore waters in the Mid-Atlantic Bight were dominated almost equally ($\pm$10%) by phytoplankton, detritus, and CDOM; however, the relative absorption of light in offshore bottom waters was dominated by CDOM. Low-salinity river plumes were best delineated by high loads of CDOM. These inverted bio-optical parameters will show utility in delineating waters masses in the nearshore coastal ocean.

References

Aarup, T., N. Holt, and N. Højerslev (1996), Optical measurements in the North Sea-Baltic Sea transition zone. II. Water mass classification along the Jutland west coast from salinity and spectral irradiance measurements, *Cont. Shelf. Res.*, 16, 1343–1353.

Alldredge, A. L., and M. W. Silver (1988), Characteristics, dynamics and significance of marine snow, *Prog. Oceanogr.*, 20, 41–82.

Alldredge, A. L., U. Passow, and B. Logan (1993), The abundance and significance of a class of large transparent organic particles in the ocean, *Deep Sea Res., Part I*, 40, 1131–1140.

Barnard, A. H., W. S. Pegau, and J. R. V. Zaneveld (1998), Global relationships of the inherent optical properties of the oceans, *J. Geophys. Res.*, 103, 24,955–24,968.

Blough, N. V., O. C. Zafririou, and J. Bonilla (1993), Optical absorption spectra of waters from the Orinoco River outflow—Terrestrial input of colored organic matter to the Carribean, *J. Geophys. Res.*, 98, 2271–2278.

Boss, E., W. S. Pegau, W. D. Gardner, J. R. V. Zaneveld, A. H. Barnard, M. S. Twardowski, G. C. Chang, and T. D. Dickey (2001), Spectral particulate attenuation and particle size distribution in the bottom boundary layer of a continental shelf, *J. Geophys. Res.*, 106, 509–516.

Bricaud, A., A. Morel, and L. Prieur (1981), Absorption by dissolved organic matter of the sea (yellow substance) in the UV and visible domains, *Limnol. Oceanogr.*, 26, 45–53.

Bricaud, A., M. Babin, A. Morel, and H. Claustre (1995), Variability in the chlorophyll-specific absorption coefficients of natural phytoplankton: Analysis and parameterization, *J. Geophys. Res.*, 100, 13,321–13,332.

Carder, K. L., R. G. Steward, G. R. Harvey, and P. B. Ortner (1989), Marine humic and fulvic acids: Their effects on remote sensing of chlorophyll *a*, *Limnol. Oceanogr.*, 34, 68–81.

Chang, G. C., and T. D. Dickey (1999), Partitioning in situ spectral absorption by use of moored spectral absorption-attenuation meters, *Appl. Opt.*, 38, 3876–3887.

Chang, G. C., T. D. Dickey, O. M. Schofield, A. D. Weidemann, E. Boss, W. S. Pegau, M. A. Moline, and S. M. Glenn (2002), Nearshore physical processes and bio-optical properties in the New York Bight, *J. Geophys. Res.*, 107(C9), 3133, doi:10.1029/2001JC001018.

Chen, R. F. (1999), In situ fluorescence of dissolved organic matter in seawater, *Mar. Chem.*, 37, 191–221.

Craghan, M. (1995), Topographic changes and sediment characteristics at a shoreface sand ridge: Beach Haven Ridge, New Jersey, M.S. thesis, Rutgers Univ., New Brunswick, N. J.

Critchley, C. (1994), D1 protein turnover: Response to photodamage or regulatory mechanism?, in *Photoinhibition of Photosynthesis From Molecular Mechanisms to the Field*, edited by N. R. Baker and J. R. Bowyer, pp. 195–201, BIOS Sci., Oxford, UK.

Cullen, J. J. (1982), The deep chlorophyll maximum: Comparing profiles of chlorophyll *a*, *Can. J. Fish. Aquat. Sci.*, 39, 791–803.

Demmig-Adams, B. (1990), Carotenoids and photoprotection: A role for the xanthophyll zeaxanthin, *Biochim. Biophys. Acta*, 1020, 1–24.

Falkowski, P. G., and D. A. Kiefer (1985), Chlorophyll *a* fluorescence and phytoplankton: Relationship to photosynthesis and biomass, *J. Plankton Res.*, 7, 715–731.

Falkowski, P. G., and J. A. Raven (1997), *Aquatic Photosynthesis*, 375 pp., Blackwell Sci., Malden, Mass.

Gallegos, C. L., and P. J. Neale (2002), Partitioning spectral absorption in case 2 waters: Discrimination of dissolved and particulate components, *Appl. Opt.*, 41, 4220–4233.

Glenn, S. M., D. B. Haidvogel, O. Schofield, J. F. Grassle, C. J. von Alt, E. R. Levine, and D. C. Webb (1998), Coastal predictive skill experiments at the LEO-15 national littoral laboratory, *Sea Tech.*, 39, 63–69.

Glenn, S., T. D. Dickey, B. Parker, and W. Boicourt (2000), Long-term real-time coastal ocean observation networks, *Oceanography*, 13, 24–34.

Glenn, S., et al. (2004), Biogeochemical impact of summertime coastal upwelling on the New Jersey Shelf, *J. Geophys. Res.*, 109, C12S02, doi:10.1029/2003JC002265.

Green, S. A., and N. V. Blough (1994), Optical absorption and fluorescence properties of chromophoric dissolved organic matter in natural waters, *Limnol. Oceanogr.*, 39, 1903–1916.

Guixa-Boixeru, N., D. Vaque, J. M. Gasol, and C. Pedros-Alio (1999), Distribution of viruses and the potential effect on bacterioplankton in an oligotrophic marine system, *Aquat. Microbiol. Ecol.*, 19, 205–213.

Højerslev, N. K., N. Holt, and T. Aarup (1996), Optical measurements in the North Sea-Baltic Sea transition zone. I. On the origin of the deep water in Kattegat, *Cont. Shelf. Res.*, 16, 1329–1342.

Jeffrey, S. W., R. F. C. Mantoura, and S. W. Wright (1997), *Phytoplankton Pigments in Oceanography*, 661 pp., U.N. Educ., Sci., and Cult. Org., Paris.

Johnson, G., O. Samset, L. Granskog, and E. Sakshaug (1994), In vivo absorption characteristics in 10 classes of bloom-forming phytoplankton: Taxonomic characteristics and responses to photoadaptation by means to discriminant and HPLC analysis, *Mar. Ecol. Prog. Ser.*, 105, 149–157.

Johnson, D. R., J. Miller, and O. Schofield (2003), Dynamics and optics of the Hudson River outflow plume, *J. Geophys. Res.*, 108(C10), 3323, doi:10.1029/2002JC001485.

Kalle, K. (1966), The problem of the gelbstoff in the sea, *Oceanogr. Mar. Biol. Rev.*, 4, 91–104.

Kiefer, D. A. (1973), Chlorophyll *a* fluorescence in marine centric diatoms: Responses of chloroplasts to light and nutrient stress, *Mar. Biol.*, 23, 39–46.

Kirk, J. T. O. (1994), *Light and Photosynthesis in Aquatic Ecosystems*, 509 pp., Cambridge Univ. Press, New York.

Kirkpatrick, G., D. F. Millie, M. A. Moline, and O. Schofield (2000), Absorption-based discrimination of phytoplankton species in naturally mixed populations, *Limnol. Oceanogr.*, 42, 467–471.

Kirkpatrick, G. J., C. Orrico, M. J. Oliver, M. A. Moline, and O. Schofield (2003), Continuous real-time determination of hyperspectral absorption of colored dissolved organic matter, *Appl. Opt.*, 42, 6564–6568.

Kishino, M., M. Takahashi, N. Okami, and S. Ichimura (1985), Estimation of the spectral absorption coefficients of phytoplankton in the sea, *Bull. Mar. Sci.*, 37, 634–642.

Komada, T., O. Schofield, and C. Reimers (2002), Fluorescence characteristics of organic matter released from coastal sediments during resuspension, *Mar. Chem.*, 79, 81–97.

Kroon, B. M. A. (1994), Variability of photosystem II quantum yields and related processes in *Chlorella pyrenoidsa* (*Chlorophyta*) acclimated to an oscillating light regime simulating a mixed photic zone, *J. Phycol.*, 30, 841–852.

Mackey, M. D., D. Mackey, H. Higgins, and S. Wright (1996), CHEMTAX—A program for estimating class abundances from chemical markers: Application to HPLC measurements of phytoplankton, *Mar. Ecol. Prog. Ser.*, 144, 265–283.

Mackey, M. D., H. W. Higgins, D. J. Mackey, and D. Holdsworth (1998), Algal class abundances in the western equatorial Pacific: Estimation from HPLC measurements of chloroplast pigments using CHEMTAX, *Deep Sea Res., Part I*, 45, 1441–1468.

Millie, D. F., O. Schofield, G. J. Kirkpatrick, G. Johnsen, P. A. Tester, and B. T. Vinyard (1997), Phytoplankton pigments and absorption spectra as

potential 'biomarkers' for harmful algal blooms: A case study of the Florida red-tide dinoflagellate, *Gymnodinium breve, Limnol. Oceanogr.*, *42*, 1240–1251.

Millie, D. F., O. Schofield, G. J. Kirkpatrick, G. Johnsen, and T. J. Evens (2002), Using absorbance and fluorescence spectra to discriminate microalgae, *Eur. J. Phycol.*, *37*, 313–322.

Mobley, C. D. (1994), *Light and Water Radiative Transfer in Natural Waters*, 591 pp., Academic, San Diego, Calif.

Moline, M. A., S. Blackwell, R. Chant, M. J. Oliver, T. Bergmann, S. Glenn, and O. M. E. Schofield (2004), Episodic physical forcing and the structure of phytoplankton communities in the coastal waters of New Jersey, *J. Geophys. Res.*, *109*, C12S05, doi:10.1029/2003JC001985.

Morel, A., and A. Bricaud (1986), Inherent optical properties of algal cells including picoplankton: Theoretical and experimental results, in *Photosynthetic Picoplankton*, edited by T. Platt and W. K. W. Li, *Can. Bull. Fish. Aquat. Sci.*, *214*, 521–559.

Nelson, N. B., and D. A. Siegel (2002), Chromophoric DOM in the open ocean, in *Biogeochemistry of Marine Dissolved Organic Matter*, pp. 547–578, Elsevier Sci., New York.

Nelson, N. B., D. A. Siegel, and A. F. Michaels (1998), Seasonal dynamics of colored dissolved organic material in the Sargasso Sea, *Deep Sea Res., Part I*, *45*, 931–957.

Nickelsen, J., and J. D. Rochaix (1994), Regulation of synthesis of D1 and D2 proteins of photosystem II., in *Photoinhibition of Photosynthesis From Molecular Mechanisms to the Field*, pp. 179–190, edited by N. R. Baker and J. R. Bowyer, BIOS Sci., Oxford, UK.

Oliver, M. J., S. Glenn, J. T. Kohut, A. J. Irwin, O. M. Schofield, M. A. Moline, and W. P. Bissett (2004a), Bioinformatic approaches for objective detection of water masses on continental shelves, *J. Geophys. Res.*, *109*, C07S04, doi:10.1029/2003JC002072.

Oliver, M. J., O. Schofield, T. Bergmann, S. Glenn, C. Orrico, and M. Moline (2004b), Deriving in situ phytoplankton absorption for bio-optical productivity models in turbid waters, *J. Geophys. Res.*, *109*, C07S11, doi:10.1029/2002JC001627.

Owens, T. G., A. P. Shreve, and A. C. Albrecht (1993), Dynamics and mechanism of singlet energy transfer between carotenoids and chlorophylls: Light-harvesting and nonphotochemical fluorescence quenching, in *Research in Photosynthesis*, vol. IV, edited by N. Murata, pp. 179–186, Kluwer Acad., Norwell, Mass.

Passow, U., A. L. Alldredge, and B. E. Logan (1994), The role of particulate carbohydrate exudates in the flocculation of diatom blooms, *Deep Sea Res., Part I*, *41*, 335–357.

Pegau, S. W., et al. (1995), A comparison of methods for the measurement of the absorption coefficient in natural waters, *J. Geophys. Res.*, *100*, 13,201–13,221.

Prasil, O., N. Adir, and I. Ohad (1992), Dynamics of photosystem II: Mechanism of photoinhibition and recovery processes, in *The Photosystems: Structure, Function and Molecular Biology*, edited by J. Barber, pp. 295–348, Elsevier, New York.

Robinson, A. R., and S. Glenn (1999), Adaptive sampling for ocean forecasting, *Nav. Res. Rev.*, *51*, 26–38.

Roelke, D. L., C. D. Kennedy, and A. D. Weidemann (1999), Use of discriminant and fourth-derivative analyses with high-resolution absorption spectra for phytoplankton research: Limitations at varied signal to noise ratio and spectral resolution, *Fish. Aquat. Ecol.*, *17*, 17–28.

Roesler, C. S. (1998), Theoretical and experimental approaches to improve the accuracy of particulate absorption coefficients derived from the quantitative filter technique, *Limnol. Oceanogr.*, *43*, 1649–1660.

Roesler, C. S., and M. J. Perry (1995), In situ phytoplankton absorption, fluorescence emission, and particulate backscattering spectra determined from reflectance, *J. Geophys. Res.*, *100*, 13,279–13,294.

Roesler, C. S., M. J. Perry, and K. L. Carder (1989), Modeling in situ phytoplankton absorption from total absorption spectra in productive inland marine waters, *Limnol. Oceanogr.*, *34*, 1510–1523.

Schofield, O., J. Gryzmski, W. P. Bissett, G. J. Kirkpatrick, D. F. Millie, M. A. Moline, and C. R. Roesler (1999), Optical monitoring and forecasting systems for harmful algal blooms: Possibility or pipedream?, *J. Phycol.*, *35*, 125–145.

Schofield, O., T. Bergmann, W. P. Bisset, F. Grassle, D. Haidvogel, J. Kohut, M. Moline, and S. Glenn (2002), The long term ecosystem observatory: An integrated coastal observatory, *IEEE J. Oceanic Eng.*, *27*, 146–154.

Tomczak, M. (1999), Some historical, theoretical and applied aspects of quantitative water mass analysis, *J. Mar. Res.*, *57*, 275–303.

Twardowski, M. S., J. M. Sullivan, P. L. Donaghay, and J. R. V. Zaneveld (1999), Microscale quantification of the absorption by dissolved and particulate material in coastal waters with an ac-9, *J. Atmos. Oceanic Technol.*, *16*, 691–707.

Twardowski, S. M., E. Boss, J. B. MacDonald, W. S. Pegau, A. H. Barnard, and J. R. V. Zaneveld (2001), A model for estimating bulk refractive index from optical backscattering ratio and implications for understanding particle composition in case I and case II waters, *J. Geophys. Res.*, *106*, 14,129–14,142.

Vodacek, A., N. V. Blough, M. D. DeGrandpre, E. T. Peltzer, and R. K. Nelson (1997), Seasonal variation of CDOM and DOC in the Middle Atlantic Bight: Terrestrial inputs and photooxidation, *Limnol. Oceanogr.*, *42*, 674–686.

Wright, S. W., S. W. Jeffrey, R. F. C. Mantoura, C. A. Llewellyn, T. Bjornland, D. Repeta, and N. Welschmeyer (1991), Improved HPLC method for the analysis of chlorophylls and carotenoids from marine phytoplankton, *Mar. Ecol. Prog. Ser.*, *77*, 183–196.

————————————

T. Bergmann, A. Irwin, M. J. Oliver, and O. Schofield, Coastal Ocean Observation Lab, Institute of Marine and Coastal Sciences, Rutgers University, New Brunswick, NJ 08901, USA. (oscar@imcs.marine.rutgers.edu)

W. P. Bissett, Florida Environmental Research Institute, 4807 Bayshore Blvd. Suite 101, Tampa, FL 33611, USA.

G. Kirkpatrick, Mote Marine Laboratory, 1600 Ken Thompson Parkway, Sarasota, FL 34236, USA.

M. A. Moline and C. Orrico, Biological Sciences Department, California Polytechnic State University, San Luis Obispo, CA 93407, USA.